Preparation and Reaction of Naked Metal Clusters for Catalysis and Genetic Materials①

CUI Chao-Nan[a②] ZHANG Han-Yu[a, b②]
LUO Zhi-Xun[a, b③] PAN Feng[c]

[a] (*Beijing National Laboratory for Molecular Sciences* (*BNLMS*)*, State Key Laboratory for Structural Chemistry of Unstable and Stable Species, Institute of Chemistry, Chinese Academy of Sciences, Beijing* 100190*, China*)

[b] (*University of Chinese Academy of Sciences, Beijing* 100049*, China*)

[c] (*School of Advanced Materials, Peking University Shenzhen Graduate School, Shenzhen* 518055*, China*)

ABSTRACT Metal clusters that contain a small number of atoms usually present unique properties with dramatic dependence on their sizes, geometric structures, and compositions. The studies of naked metal clusters are devoted to develop new catalysts and functional materials of atomic precision, and enable to improve the fundamental theory of structure chemistry and to understand the basic reactions and properties bridging the gap between atoms and bulk materials. In particular, some interesting superatom clusters have received reasonable research interest indicative of materials gene of clusters. Here in this review, we simply summarize the preparation, stability, and reactivity of naked metal clusters with a few examples displayed. Hopefully it serves as a modest spur to stimulate more interest of related investigations in this field.

Keywords: metal clusters, structure chemistry, superatom, cluster reactivity;
DOI: 10.14102/j.cnki.0254-5861.2011-2886

1 INTRODUCTION

When the size of metal particles is reduced to a few nanometers small enough to approach the de Broglie wavelength of electrons, unusual quantum-sized properties, such as ultra-high catalytic activity, dramatic optical, electronic and magnetic properties, could be achieved[1, 2]. The distinct performance of metal clusters at sub-nano scale is due to a variety of factors including large surface to bulk ratio and quantum confinement, which has a strong correlation with the cluster size, geometric/electronic structures and compositions[3, 4]. Over the last fifty years, considerable interest has been attracted in metal clusters. Various metal clusters protected by ligand monolayers have been synthesized, and their stabilities are often rationalized by a superatom characteristic of the metallic core. A majority of the monolayer-protected clusters (MPCs) finds core-shell structures[5, 6], with several types of fundamental building blocks having been identified, including tetrahedral M_4[7, 8], octahedral M_6[9], bi-tetrahedral M_8[10], hollow-cage M_{12}[11-13], and in particular icosahedral M_{13}[14]. For example, a variety of MPCs like Au_{18}[15], Au_{20}[16, 17], Au_{25}[18], Au_{30}[19, 20], Au_{36}[21, 22], Au_{38}[23], Au_{55}[24-26], Au_{60}[27], Au_{102}[28] and so on have a 13-atom icosahedral inner core[29, 30]. The MPCs find enhanced stability in the presence of a superatom metallic kernel, and novel ligand-metal interaction could result in electronic accommodation enabling a transition from planar to three-dimensional structure[31-36]. For example, planar Au_{13} has a local minima energy while $Al_{13}(SR)_x$ an icosahedral core[37, 38]. Even so, the nature of the metallic core is believed to play a determining role in the cluster structure evolution[39], stability and electronic transition between frontier orbitals. Note that, the metal-metal bonding is weaker than ionic and covalent bonds, and the valence electrons of metal often occupy the higher energy levels of the cluster. It is unequivocally significant for insightful studies of naked metal clusters pertaining to catalysis and genetic materials.

Received 20 May 2020; accepted 3 June 2020
① This work was financially supported by the National Natural Science Foundation of China (Nos. 21802146 and 21722308), CAS Key Research Project of Frontier Science (CAS Grant QYZDB-SSW-SLH024), and Frontier Cross Project of National Laboratory for Molecular Sciences (051Z011BZ3)
② These authors contribute equally to this work
③ Corresponding author. Luo Zhi-Xun. E-mail: zxluo@iccas.ac.cn

To study the chemistry of naked metal clusters, the prime object is to generate pure metal clusters in gas-phase experiments. With the development of supersonic expansion and molecule beam technique which became mature since 1980s, a variety of cluster sources have been used to form metal clusters[40]. Based on the studies of gas phase reactions, interestingly some naked metal clusters with specific geometry and electronic configurations can achieve outstanding stability or size-dependent reactivity, which is often understood with in the conceptual framework of superatoms[14, 41-44]. Also, extensive investigations of metal cluster reactivity have been conducted by theoretical methods[40, 45-48]. In this mini review, we simply summarize the recent advances of instrument and technique for metal cluster preparation, stability, and reactivity with a few examples in our own group. It is anticipated to appeal to colleagues to contribute more future investigations to metal cluster chemistry and genetic materials.

2 PREPARATION OF NAKED METAL CLUSTERS

Metal clusters in gas phase have become the ideal model for studying the structure and reaction mechanism because of its definite and controllable atomic composition. However, the preparation of naked metal clusters is challenging because the strength of metal-oxygen bond is much larger than that of metal-metal bond[49-51], and the interference of oxygen in system will block the generation of naked metal clusters. Instead, metal oxide clusters are relatively easier formed in gas phase experiments[52]. Among the approaches available for cluster generation, the laser-vaporization source (LaVa-source, also known as "Smalley source")[53, 54] is mostly used as a convenient and highly flexible method. However, subject to the single-photon energy of ionization laser, the formation of neutral metal cluster is a larger challenge. Recently, uprising research interest has been attracted by a magnetron sputtering source (MagS-source, also known as gas condensation source)[55-58], which takes advantages of high efficiency and controllability. Among others, thermal heated oven sources (also known as Knudsen ovens)[59-64] and pulsed arc-discharge method (also known as pick-up source)[65, 66] are also available for the production of different metal clusters in the gas phase. Besides, electrospray ionization (ESI)[67-69] is known as a mild ionization technology of solution samples applicable for observing MPCs synthesized in wet chemistry.

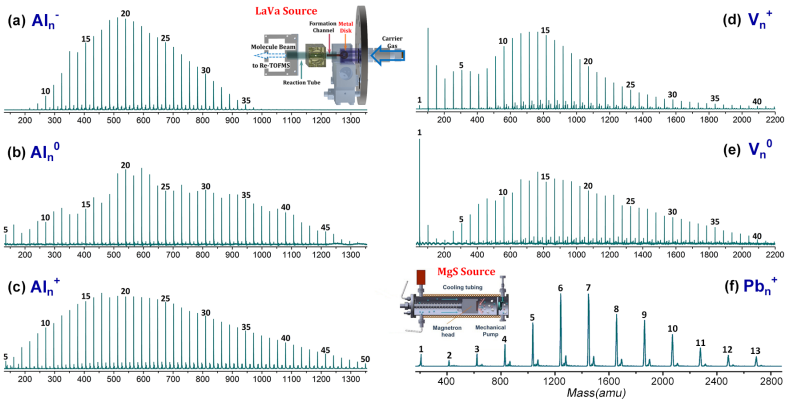

Fig. 1. Typical mass distributions of the naked metal clusters prepared by a LaVa source (a～e) and a MagS source (f)

Recently we have got an improvement in the instrumentation to prepare well-resolved naked metal clusters[70]. Fig. 1a～1c display the anionic, neutral and cationic aluminum clusters generated by our homemade LaVa-source, where the 532 nm laser (Nd: YAG, 10 Hz) was focused onto a translational and rotational motion metal disk in the presence of high purity helium as carrier gas which is controlled by a pulsed general valve. The molecular beam, of which the charged species can be deflected (optional for neutral cluster study) by an electric field located downstream of the fast-flow reactor, then enters into the second chamber for mass analysis[71]. Similarly, Fig. 1d and 1e present the typical mass distributions of the vanadium clusters. It is notable that, as vanadium is more readily contaminated with oxygen, the preparation of naked metal clusters of such metals is not a trivial. Besides, MagS source is also available for the preparation of naked metal clusters. A typical example is shown in Fig. 1f.

In general, the influences of the nozzle length and inner dimeter of cluster formation channel, vacuum degree, and

relative background pressure need to be meticulously evaluated and repeatedly tested in order to prepare well-resolved pure metal clusters. When the length of cluster formation channel is increased, larger metal cluster can be attained by slightly decreasing the inner dimeter and simultaneously increasing the background pressure. It is notable that vacuum degree is an important parameter to avoid oxygen contaminations. Furthermore, benefited from the development of deep ultraviolet laser source (DUV)[72] of which the single-photon energy is up to 7 eV, the neutral metal clusters have been successfully prepared (Fig. 1b and 1e). Well-resolved pure metal clusters (Fig. 1) promote the research in the fields of metal cluster reactivity and stability[40, 70, 73-76].

3 PROBING CLUSTER STABILITY AND SUPERATOM CHARACTERISTICS

The research interest in probing the gas-phase metal cluster stability can be traced back to 1980s when "magic numbers" in the mass spectra of free sodium clusters were observed by Knight and co-workers[77]. Following that, ongoing efforts are devoted to studying metal cluster stability by measuring the relative mass abundances of clusters formed in comparable conditions using mass spectrometry, by further reacting with oxygen or other appropriate reactants, or by evaluating the size-dependent reactivity of mass-selected clusters[78, 79]. Based on near-free electron gas (NFEG) theory, a "jellium model" is used to account for the enhanced stability of these specific metal clusters[43, 80-86]. Within this jellium model, metal clusters with closed electronic shells often exhibit a large HOMO-LUMO gap, hence enhancing the stability and reducing the reactivity. However, not all metal clusters are subject to the same fundamental constraints. For example, metal clusters of favorable geometry within Mackay icosahedrons often find prominent stability[87]. On this basis, stable clusters are anticipated to be associated with a geometric and/or electronic shell closure[4, 43, 86].

The novelty of metal cluster chemistry is far more than the discovery of stable species with regular structures hence to understand how they are chemical alert; instead, it enables to create new materials which consist of clusters instead of atoms as building blocks. The cluster-genetic materials based on superatoms could fuel the hope to synthesize materials from the bottom-up with atomic precision and unique tailored properties as a function of size, shape, and composition. For example, a magic cluster Al_{13}^- having both an electronic and a geometric shell closure structures was found to be resistant to oxygen etching[88], as shown in Fig. 2a. The electronic levels in Al_{13}^- correspond to $|1S^2|1P^6|1D^{10}2S^2|2P^61F^{14}||2D^01G^0|$ shell structure, which is similar to the atomic orbitals of Cl^-. Further insights into Al-based cluster reactivity have also been attained for Al-Mg alloy metal clusters (Fig. 2b)[89]. Considering magnesium is divalent and aluminum is trivalent, the Al-Mg alloy clusters actually offer larger variations over the electron counts than pure aluminum clusters. As shown in Fig. 2d, the HOMO-LUMO gaps also account for their relative stability as functions of the number of valence electrons and associate with their electronic configuration and superatom orbital characteristics. Specifically, largely delocalized electron cloud density gives rise to significant superatom orbital characteristics pertaining to all-metal aromaticity[90] which, in turn, enhances the cluster stability. Some other metal clusters such as Ag_{13}^- also exhibit enhanced stability and superatom orbital patterns, although their lowest energy structures are not icosahedral[91, 92].

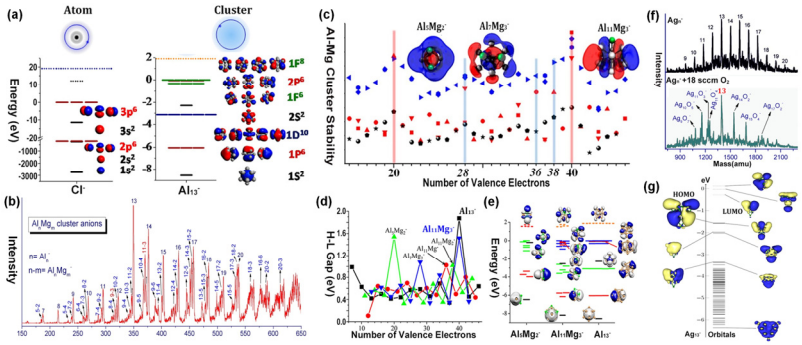

Fig. 2. (a) Electronic structure and atomic and molecular orbitals of Cl^- and Al_{13}^-[86]. (b) Mass spectrum of $Al_nMg_m^-$ anions[89]. (c) Al-Mg cluster stability corresponding to the number of valence electrons. (d) Calculated HOMO-LUMO gaps of $Al_nMg_m^-$ plotted versus the number of valence electrons. (e) Molecular orbital diagrams of $Al_5Mg_2^-$, $Al_{11}Mg_3^-$, and Al_{13}^-. (f) Mass spectra of silver cluster anions (Ag_n^-) produced via a MagS source after exposure to oxygen[91]. (g) Calculated molecular orbitals of Ag_{13}^-

4 REACTIVITY AND CATALYSIS

4. 1 Gas-phase reactions of naked metal clusters

Metal cluster reactions with small molecules cannot only provide insights into the reactivity and property of metals at reduced sizes, but also facilitate the comprehensive understanding of condensed phase physics and surface chemistry[40]. In general, as indicated by the even-odd oscillations of HOMO-LUMO gaps, binding energies, ionization energies, etc. of the metal clusters, the metal cluster reactivity generally undergoes odd-even alternation effect especially for the charge-transfer dominated reactions. Besides, certain reactions of the metal clusters could exhibit strong size-dependence and charge-state variation; also, some could be ADE-dependent reactions, with likely long-range charge transfer corresponding to the harpoon mechanism. Besides, the multiple valence states could account for the redox reactions of metal clusters with oxygenic chemicals[70, 73, 74]. For example, the transition metal vanadium has diverse valence state ranging from -1 to +5, which allows various $V_nO_m^+$ clusters to be produced in the reaction of "$V_n^+ + O_2$". It is notable that, for such transition metals, both the oxygen-etching and oxygen-addition mechanisms could coexist in the gas-phase experiments, rendering a complex mechanism of their reactivity with oxygen.

Extensive experimental and theoretical investigations have also been conducted for metal clusters reacting with water due to the importance of hydrogen evolution[93-97]. A typical example illustrated the size effect of aluminum cluster anion in reacting with water[98], where Al_{12}^- was found to be the smallest cluster that can react with water to form an adsorptive product; in comparison, a few clusters like Al_{16}^-, Al_{17}^- and Al_{18}^- can produce H_2 by reacting with multiple water. It demonstrated that the dissociation of water to form H_2 on gas-phase aluminum anion clusters can be facilitated by collaborative effect of the Lewis acid and Lewis base sites. Furthermore, complementary active Lewis acid/base sites, resulting from irregular charge distribution on the cluster surface, account for the size-dependent reactivity of aluminum clusters with water. Similar hydrogen evolution reactions have also been found for aluminum clusters reacting with alcohols[99], allowing for a competition and likely self-catalysis in the presence of multiple -OH reactants.

Besides, the reactivity of thiols with metal clusters provided an insight into the C–S bond activation[100, 101]. As ethanethiol is used as a typical reagent of thiol groups in chemical synthesis, many studies have examined the reactivity of ethanethiol with gas-phase metal clusters. A study of the Ag_n^- clusters reacting with ethanethiol showed that, the clusters of an even number of silver atoms are more reactive than those with an odd number, indicating the Ag_n^- clusters with an unpaired electron can react more readily toward ethanethiol due to the facile metal-to-thiol electron transfer interactions[101]. For cluster reaction with chlorine, the joint experimental and theoretical studies revealed that Cu_8^- and Ag_8^- clusters have high reactivity with chlorine through a novel harpoon mechanism[102]. Besides the strong charge transfer in forming ionic and covalent bonds, relative weak cluster-π interactions could also cause size-dependent reactivity of metal clusters[75, 103, 104]. For example, a recent study of Ag_n^+ clusters reacting with acetylene found that only $Ag_7^+[C_2H_2]$ was observed as the reaction product in the rich-pressure collision conditions. Analysis based on DFT calculations found that $Ag_7^+[C_2H_2]$ bears larger binding energy than the other $Ag_n^+[C_2H_2]$, that is, a minor difference of the cluster structure causes significantly altered cluster-π interaction, thus enabling to screen out the clusters with only one-atom difference[105].

4. 2 Catalysis of supported metal clusters

Supported metal catalysts have been wildly used in industrial processes due to the excellent performance for enhancing reaction efficiency, but the fundamental mechanism is too complicated to be elucidated as in real situation[1, 106]. By soft-landing deposition, selected metal clusters on support can provide an essential way to exploit the interface interactions, which is an attractive strategy to improve the catalytic reaction selectivity and efficiency of the catalysts. Much recent work has focused on studying the catalysis of size-selected metal clusters supported on different substrates[47, 107-112]. For example, S. Vajda and co-workers[113-116], J. Laskin and G. Johnson et al.[117] conducted investigations to figure out the size effect of supported clusters for many chemical reactions. It was shown that the size-selected Ag_3 clusters on alumina supports exhibit a high activity for direct propylene epoxidation with only a negligible amount of CO_2 formation at low temperature, which is benefit from the open-shell nature of the cluster electronic structure[118]. Such small cluster catalysis is believed to stimulate more research interest in this field[119, 120]. Also it was found that graphene

sheet's dephasing lengths increased in the presence of Pd cluster deposition[121], and the size of supported Pd_n clusters can affect the reactivity for electrochemical water oxidation[122], where Pd_4 has no reaction while the soft-landed Pd_6 and Pd_{17} clusters achieve the reactivity equal to the most active catalysts known. Among others, R. G. Cooks[123], A. Nakajima[124] and U. Heiz[125-127] studied the different-sized metal clusters on supports for hydrogenation reaction, oxygen reduction reaction and so forth, revealing the dramatic size-dependence of metal cluster catalysis and opening up a new method for future catalyst design.

5 SUMMARY AND PERSPECTIVE

In summary, naked metal clusters in gas phase and on solid support provide an ideal model for studying the catalytic activity, electronic and magnetic properties, and atomically precise reaction mechanisms. The development of mass spectrometry, cluster generation and soft-landing deposition methods enable to prepare a variety of naked metal clusters with diverse stability and properties. Insights obtained from superatom chemistry enable to tailor unique reactivity and electronic properties of metal clusters, promoting the potential applications of naked metal clusters as catalysts and genetic materials. Furthermore, the chemical interactions, electronic structures and specific sizes affect the affinities and reactivities of metal clusters toward specific reactants, giving rise to better understanding of the fundamentals involved in many metal-related chemical processes, including catalysis, crystal nucleation and growth, phase transformation and combustion. Looking forward, reasonable efforts will be paid to highly-efficient and large-scale preparation of naked metal clusters in order to realize practical applications of size-selected and structure-determined functional cluster materials.

REFERENCES

(1) Liu, L.; Corma, A. Metal catalysts for heterogeneous catalysis: from single atoms to nanoclusters and nanoparticles. *Chem. Rev.* **2018**, 118, 4981–5079.

(2) Takahashi, K.; Takahashi, L. Data driven determination in growth of silver from clusters to nanoparticles and bulk. *J. Phys. Chem. Lett.* **2019**, 10, 4063–4068.

(3) Tyo, E. C.; Vajda, S. Catalysis by clusters with precise numbers of atoms. *Nat. Nanotechnol.* **2015**, 10, 577–588.

(4) Jena, P.; Sun, Q. Super atomic clusters: design rules and potential for building blocks of materials. *Chem. Rev.* **2018**, 118, 5755–5780.

(5) Jiang, D. E.; Tiago, M. L.; Luo, W.; Dai, S. The "staple" motif: a key to stability of thiolate-protected gold nanoclusters. *J. Am. Chem. Soc.* **2008**, 130, 2777–2779.

(6) Hu, G.; Jin, R.; Jiang, D. E. Beyond the staple motif: a new order at the thiolate-gold interface. *Nanoscale* **2016**, 8, 20103–20110.

(7) Chevrier, D. M.; Zeng, C.; Jin, R.; Chatt, A.; Zhang, P. Role of au4 units on the electronic and bonding properties of $Au_{28}(SR)_{20}$ nanoclusters from X-ray spectroscopy. *J. Phy. Chem. C* **2014**, 119, 1217–1223.

(8) Tlahuice-Flores, A. New polyhedra approach to explain the structure and evolution on size of thiolated gold clusters. *J. Phy. Chem. C* **2019**, 123, 10831–10841.

(9) Yang, H.; Lei, J.; Wu, B.; Wang, Y.; Zhou, M.; Xia, A.; Zheng, L.; Zheng, N. Crystal structure of a luminescent thiolated ag nanocluster with an octahedral $Ag_6(4+)$ core. *Chem. Commun.* (*Camb*) **2013**, 49, 300–302.

(10) Song, Y.; Wang, S.; Zhang, J.; Kang, X.; Chen, S.; Li, P.; Sheng, H.; Zhu, M. Crystal structure of selenolate-protected $Au_{24}(SeR)_{20}$ nanocluster. *J. Am. Chem. Soc.* **2014**, 136, 2963–2965.

(11) Harkness, K. M.; Tang, Y.; Dass, A.; Pan, J.; Kothalawala, N.; Reddy, V. J.; Cliffel, D. E.; Demeler, B.; Stellacci, F.; Bakr, O. M. $Ag_{44}(SR)_{30}^{4-}$: a silver-thiolate superatom complex. *Nanoscale* **2012**, 4, 4269–4274.

(12) Yang, H.; Wang, Y.; Huang, H.; Gell, L.; Lehtovaara, L.; Malola, S.; Hakkinen, H.; Zheng, N. All-thiol-stabilized Ag_{44} and $Au_{12}Ag_{32}$ nanoparticles with single-crystal structures. *Nat. Commun.* **2013**, 4, 2422.

(13) Yuan, S. F.; Xu, C. Q.; Li, J.; Wang, Q. M. A ligand-protected golden fullerene: the dipyridylamido Au_{32}^{8+} nanocluster. *Angew. Chem. Int. Ed.* **2019**, 5906–5909.

(14) Jia, Y.; Luo, Z. Thirteen-atom metal clusters for genetic materials. *Coord. Chem. Rev.* **2019**, 400, 213053.

(15) Chen, Y.; Zeng, C.; Liu, C.; Kirschbaum, K.; Gayathri, C.; Gil, R. R.; Rosi, N. L.; Jin, R. Crystal structure of barrel-shaped chiral Au_{130}(p-mbt)$_{50}$ nanocluster. *J. Am. Chem. Soc.* **2015**, 137, 10076–10079.

(16) Wan, X. K.; Lin, Z. W.; Wang, Q. M. Au_{20} nanocluster protected by hemilabile phosphines. *J. Am. Chem. Soc.* **2012**, 134, 14750–14752.

(17) Zeng, C. J.; Liu, C.; Chen, Y. X.; Rosi, N. L.; Jin, R. C. Gold-thiolate ring as a protecting motif in the $Au_{20}(SR)_{16}$ nanocluster and implications. *J. Am. Chem. Soc.* **2014**, 136, 11922–11925.

(18) Zhu, M.; Aikens, C. M.; Hollander, F. J.; Schatz, G. C.; Jin, R. Correlating the crystal structure of a thiol-protected Au_{25} cluster and optical properties. *J. Am. Chem. Soc.* **2008**, 130, 5883–5885.

(19) Crasto, D.; Malola, S.; Brosofsky, G.; Dass, A.; Hakkinen, H. Single crystal XRD structure and theoretical analysis of the chiral $Au_{30}S(S\text{-}t\text{-}Bu)_{18}$ cluster. *J. Am. Chem. Soc.* **2014**, 136, 5000–5005.

(20) Yang, H. Y.; Wang, Y.; Edwards, A. J.; Yan, J. Z.; Zheng, N. F. High-yield synthesis and crystal structure of a green Au_{30} cluster co-capped by thiolate and sulfide. *Chem. Commun.* **2014**, 50, 14325–14327.

(21) Zeng, C. J.; Qian, H. F.; Li, T.; Li, G.; Rosi, N. L.; Yoon, B.; Barnett, R. N.; Whetten, R. L.; Landman, U.; Jin, R. C. Total structure and electronic properties of the gold nanocrystal $Au_{36}(SR)_{24}$. *Angew. Chem. Int. Ed.* **2012**, 51, 13114–13118.

(22) Das, A.; Liu, C.; Zeng, C. J.; Li, G.; Li, T.; Rosi, N. L.; Jin, R. C. Cyclopentanethiolato-protected $Au_{36}(SC_5H_9)_{24}$ nanocluster: crystal structure and implications for the steric and electronic effects of ligand. *J. Phys. Chem. A* **2014**, 118, 8264–8269.

(23) Qian, H. F.; Eckenhoff, W. T.; Zhu, Y.; Pintauer, T.; Jin, R. C. Total structure determination of thiolate-protected au_{38} nanoparticles. *J. Am. Chem. Soc.* **2010**, 132, 8280–8281.

(24) Boyen, H. G.; Kastle, G.; Weigl, F.; Koslowski, B.; Dietrich, C.; Ziemann, P.; Spatz, J. P.; Riethmuller, S.; Hartmann, C.; Moller, M.; Schmid, G.; Garnier, M. G.; Oelhafen, P. Oxidation-resistant gold-55 clusters. *Science* **2002**, 297, 1533–1536.

(25) Turner, M.; Golovko, V. B.; Vaughan, O. P. H.; Abdulkin, P.; Berenguer-Murcia, A.; Tikhov, M. S.; Johnson, B. F. G.; Lambert, R. M. Selective oxidation with dioxygen by gold nanoparticle catalysts derived from 55-atom clusters. *Nature* **2008**, 454, 981–983.

(26) Chang, C. M.; Cheng, C.; Wei, C. M. Co oxidation on unsupported Au_{55}, Ag_{55}, and $Au_{25}Ag_{30}$ nanoclusters. *J. Chem. Phys.* **2008**, 128, 124710.

(27) Song, Y.; Fu, F.; Zhang, J.; Chai, J.; Kang, X.; Li, P.; Li, S.; Zhou, H.; Zhu, M. The magic Au_{60} nanocluster: a new cluster-assembled material with five Au_{13} building blocks. *Angew. Chem. Int. Ed.* **2015**, 54, 8430–8434.

(28) Jadzinsky, P. D.; Calero, G.; Ackerson, C. J.; Bushnell, D. A.; Kornberg, R. D. Structure of a thiol monolayer-protected gold nanoparticle at 1.1 angstrom resolution. *Science* **2007**, 318, 430–433.

(29) Schmid, G. The relevance of shape and size of Au_{55} clusters. *Chem. Soc. Rev.* **2008**, 37, 1909–1930.

(30) Shichibu, Y.; Suzuki, K.; Konishi, K. Facile synthesis and optical properties of magic-number Au_{13} clusters. *Nanoscale* **2012**, 4, 4125–4129.

(31) Wang, J. L.; Wang, G. H.; Zhao, J. J. Density-functional study of Au-n (n = 2～20) clusters: lowest-energy structures and electronic properties. *Phys. Rev. B* **2002**, 66, 035418.

(32) Zhao, J.; Yang, J. L.; Hou, J. G. Theoretical study of small two-dimensional gold clusters. *Phys. Rev. B* **2003**, 67, 085404.

(33) Xiao, L.; Tollberg, B.; Hu, X. K.; Wang, L. C. Structural study of gold clusters. *J. Chem. Phys.* **2006**, 124, 114309.

(34) Gruber, M.; Heimel, G.; Romaner, L.; Bredas, J. L.; Zojer, E. First-principles study of the geometric and electronic structure of Au(13) clusters: importance of the prism motif. *Phys. Rev. B* **2008**, 77, 165411.

(35) Shafai, G.; Hong, S.; Bertino, M.; Rahman, T. S. Effect of ligands on the geometric and electronic structure of Au-13 clusters. *J. Phys. Chem. C* **2009**, 113, 12072–12078.

(36) Ding, W.; Huang, C.; Guan, L.; Liu, X.; Luo, Z.; Li, W. Water-soluble Au 13 clusters protected by binary thiolates: structural accommodation and the use for chemosensing. *Chem. Phys. Lett.* **2017**, 676, 18–24.

(37) Vandervelden, J. W. A.; Vollenbroek, F. A.; Bour, J. J.; Beurskens, P. T.; Smits, J. M. M.; Bosman, W. P. Gold clusters containing bidentate phosphine-ligands - preparation and X-ray structure investigation of $Au_5(dppmH)_3(dppm)(NO_3)_2$ and $Au_{13}(dppmH)_6(NO_3)_n$. *Recl. Trav. Chim. Pays-Bas* **1981**, 100, 148–152.

(38) Briant, C. E.; Theobald, B. R. C.; White, J. W.; Bell, L. K.; Mingos, D. M. P.; Welch, A. J. Synthesis and X-ray structural characterization of the centered icosahedral gold cluster compound $Au_{13}(PMe_2Ph)_{10}C_{l2}(PF_6)_3$ - the realization of a theoretical prediction. *J. Chem. Soc., Chem. Commun.* **1981**, 201–202.

(39) Zhang, H.; Reber, A. C.; Geng, L.; Rabayda, D.; Wu, H.; Luo, Z.; Yao, J.; Khanna, S. N. Formation of $Al^+(C_6H_6)_{13}$: the origin of magic number in metal-benzene clusters determined by the nature of the core. *CCS Chemistry* **2019**, 1, 571–581.

(40) Luo, Z.; Castleman, A. W. Jr.; Khanna, S. N. Reactivity of metal clusters. *Chem. Rev.* **2016**, 116, 14456–14492.

(41) Zhang, X.; Wang, Y.; Wang, H.; Lim, A.; Gantefoer, G.; Bowen, K. H.; Reveles, J. U.; Khanna, S. N. On the existence of designer magnetic

superatoms. *J. Am. Chem. Soc.* **2013**, 135, 4856–4861.

(42) Imaoka, T.; Kitazawa, H.; Chun, W. J.; Omura, S.; Albrecht, K.; Yamamoto, K. Magic number Pt-13 and misshapen Pt-12 clusters: which one is the better catalyst? *J. Am. Chem. Soc.* **2013**, 135, 13089–13095.

(43) Luo, Z.; Castleman, A. W. Special and general superatoms. *Acc. Chem. Res.* **2014**, 47, 2931–2940.

(44) Wu, H. M.; Luo, Z. X. Chlorine-passivated superatom Al_{37} clusters for nonlinear optics. *Sci. China-Chem.* **2018**, 61, 1619–1623.

(45) Chen, J.; Luo, Z.; Yao, J. Theoretical study of tetrahydrofuran-stabilized Al_{13} superatom cluster. *J. Phys. Chem. A* **2016**, 120, 3950–3957.

(46) Pembere, A. M.; Luo, Z. X. Jones oxidation of glycerol catalysed by small gold clusters. *Phys. Chem. Chem. Phys.* **2017**, 19, 6620–6625.

(47) Negreiros, F. R.; Halder, A.; Yin, C. R.; Singh, A.; Barcaro, G.; Sementa, L.; Tyo, E. C.; Pellin, M. J.; Bartling, S.; Meiwes-Broer, K. H.; Seifert, S.; Sen, P.; Nigam, S.; Majumder, C.; Fukui, N.; Yasumatsu, H.; Vajda, S.; Fortunelli, A. Bimetallic Ag-Pt sub-nanometer supported clusters as highly efficient and robust oxidation catalysts. *Angew. Chem. Int. Ed.* **2018**, 57, 1209–1213.

(48) Ren, Y.; Yang, Y.; Zhao, Y. X.; He, S. G. Size-dependent reactivity of rhodium cluster anions toward methane. *J. Phy. Chem. C* **2019**, 123, 17035–17042.

(49) Huheey, J. E.; Cottrell, T. L. *The Strengths of Chemical Bonds*. 2nd ed ed. Academic Press: Butterworths, London **1958**.

(50) Kerr, J. A. Bond dissociation energies by kinetic methods. *Chem. Rev.* **1966**, 66, 465–500.

(51) Haynes, W. M. *Crc Handbook of Chemistry and Physics*. 95th ed.; CRC press **2014**.

(52) Yuan, Z.; Liu, Q. Y.; Li, X. N.; He, S. G. Formation, distribution, and photoreaction of nano-sized vanadium oxide cluster anions. *Int. J. Mass Spectrom.* **2016**, 407, 62–68.

(53) Dietz, T. G.; Duncan, M. A.; Powers, D. E.; Smalley, R. E. Laser production of supersonic metal cluster beams. *J. Chem. Phys.* **1981**, 74, 6511–6512.

(54) Geusic, M. E.; Morse, M. D.; O'Brien, S. C.; Smalley, R. E. Surface reactions of metal clusters i: the fast flow cluster reactor. *Rev. Sci. Instrum.* **1985**, 56, 2123–2130.

(55) Haberland, H.; Karrais, M.; Mall, M.; Thurner, Y. Thin films from energetic cluster impact: a feasibility study. *J. Vac. Sci. Technol. A* **1992**, 10, 3266–3271.

(56) Goldby, I. M.; vonIssendorff, B.; Kuipers, L.; Palmer, R. E. Gas condensation source for production and deposition of size-selected metal clusters. *Rev. Sci. Instrum.* **1997**, 68, 3327–3334.

(57) Pratontep, S.; Carroll, S. J.; Xirouchaki, C.; Streun, M.; Palmer, R. E. Size-selected cluster beam source based on radio frequency magnetron plasma sputtering and gas condensation. *Rev. Sci. Instrum.* **2005**, 76, 045103.

(58) Luo, Z.; Woodward, W. H.; Smith, J. C.; Castleman, A. W. Jr. Growth kinetics of al clusters in the gas phase produced by a magnetron-sputtering source. *Int. J. Mass Spectrom.* **2012**, 309, 176–181.

(59) Larsen, R. A.; Neoh, S. K.; Herschbach, D. R. Seeded supersonic alkali atom beams. *Rev. Sci. Instrum.* **1974**, 45, 1511–1516.

(60) Preuss, D. R.; Pace, S. A.; Gole, J. L. Supersonic expansion of pure copper vapor. *J. Chem. Phys.* **1979**, 71, 3553–3560.

(61) Sattler, K.; Muhlbach, J.; Recknagel, E. Generation of metal-clusters containing from 2 to 500 atoms. *Phys. Rev. Lett.* **1980**, 45, 821–824.

(62) Riley, S. J.; Parks, E. K.; Mao, C. R.; Pobo, L. G.; Wexler, S. Generation of continuous beams of refractory-metal clusters. *J. Phys. Chem.* **1982**, 86, 3911–3913.

(63) Knight, W. D.; Clemenger, K.; Deheer, W. A.; Saunders, W. A.; Chou, M. Y.; Cohen, M. L. Electronic shell structure and abundances of sodium clusters. *Phys. Rev. Lett.* **1984**, 52, 2141–2143.

(64) Han, K. L.; Lu, R. C.; Lin, H.; Gallogy, E. B.; Jackson, W. M. Formation of a supersonic beam of $C_{60}H_{2x}$ in a knudsen oven source containing C60 and hydrogen. *Chem. Phys. Lett.* **1995**, 243, 29–35.

(65) Satoh, N.; Kimura, K. High-resolution solid-state nmr in liquids. 2. Aluminum-27 nmr study of aluminum trifluoride ultrafine particles. *J. Am. Chem. Soc.* **1990**, 112, 4688–4692.

(66) Haberland, H. *Clusters of Atoms and Molecules: Theory, Experiment, and Clusters of Atoms*. Springer-Verlag **1994**, p422.

(67) Dole, M.; Mack, L. L.; Hines, R. L.; Mobley, R. C.; Ferguson, L. D.; Alice, M. B. Molecular beams of macroions. *J. Chem. Phys.* **1968**, 49, 2240–2249.

(68) Yamashita, M.; Fenn, J. B. Electrospray ion-source - another variation on the free-jet theme. *J. Phys. Chem.* **1984**, 88, 4451–4459.

(69) Whitehouse, C.; Dreyer, R.; Yamashita, M.; Fenn, J. B. Electrospray interface for liquid chromatographs and mass spectrometers. *Anal. Chem.* **1985**, 57, 675–679.

(70) Zhang, H.; Wu, H.; Jia, Y.; Geng, L.; Luo, Z.; Fu, H.; Yao, J. An integrated instrument of DUV-IR photoionization mass spectrometry and spectroscopy for neutral clusters. *Rev. Sci. Instrum.* **2019**, 90, 073101.

(71) Duncan, M. A. Invited review article: laser vaporization cluster sources. *Rev. Sci. Instrum.* **2012**, 83, 041101.

(72) Yuan, C.; Liu, X.; Zeng, C.; Zhang, H.; Jia, M.; Wu, Y.; Luo, Z.; Fu, H.; Yao, J. All-solid-state deep ultraviolet laser for single-photon ionization mass spectrometry. *Rev. Sci. Instrum.* **2016**, 87, 024102.

(73) Armstrong, A.; Zhang, H.; Reber, A. C.; Jia, Y.; Wu, H.; Luo, Z.; Khanna, S. N. Al valence controls the coordination and stability of cationic aluminum-oxygen clusters in reactions of Al_n^+ with oxygen. *J. Phys. Chem. A* **2019**, 123, 7463–7469.

(74) Zhang, H.; Wu, H.; Geng, L.; Jia, Y.; Yang, M.; Luo, Z. Furthering the reaction mechanism of cationic vanadium clusters towards oxygen. *Phys. Chem. Chem. Phys.* **2019**, 21, 11234–11241.

(75) Yang, M.; Zhang, H.; Jia, Y.; Yin, B.; Luo, Z. Charge-sensitive cluster-π interactions cause altered reactivity of $Al_n^{\pm, 0}$ clusters with benzene: enhanced stability of Al_{13}^+bz. *J. Phys. Chem. A* **2020**.

(76) Yang, M.; Wu, H.; Huang, B.; Luo, Z.; Hansen, K. Iodization threshold in size-dependent reactions of lead clusters Pb_n^+ with iodomethane. *J. Phys. Chem. A* **2020**, 124, 2505–2512.

(77) Knight, W. D.; Clemenger, K.; de Heer, W. A.; Saunders, W. A.; Chou, M. Y.; Cohen, M. L. Electronic shell structure and abundances of sodium clusters. *Phys. Rev. Lett.* **1984**, 52, 2141–2143.

(78) Brack, M. The physics of simple metal clusters: self-consistent jellium model and semiclassical approaches. *Rev. Mod. Phys.* **1993**, 65, 677–732.

(79) de Heer, W. A. The physics of simple metal clusters: experimental aspects and simple models. *Rev. Mod. Phys.* **1993**, 65, 611–676.

(80) Cha, C. Y.; Ganteför, G.; Eberhardt, W. Photoelectron spectroscopy of Cu-n clusters: comparison with jellium model predictions. *J. Chem. Phys.* **1993,** 99, 6308–6312.

(81) King, R. B.; Zhao, J. The isolable matryoshka nesting doll icosahedrql cluster As@Ni–12@As–20 (3-) as a "superatom": analogy with the jellium cluster Al-13(-) generated in the gas phase by laser vaporization. *Chem. Commun.* **2006**, 4204–4205.

(82) Jones, C. E. Jr.; Clayborne, P. A.; Reveles, J. U.; Melko, J. J.; Gupta, U.; Khanna, S. N.; Castleman, A. W. Al(n)bi clusters: transitions between aromatic and jellium stability. *J. Phys. Chem. A* **2008**, 112, 13316–13325.

(83) King, R. B.; Silaghi-Dumitrescu, I. The role of "external" lone pairs in the chemical bonding of bare post-transition element clusters: the wade-mingos rules versus the jellium model. *Dalton Trans.* **2008**, 44, 6083–6088.

(84) Polozkov, R. G.; Ivanov, V. K.; Verkhovtsev, A. V.; Solov'yov, A. V. Stability of metallic hollow cluster systems: Jellium model approach. *Phys. Rev. A* **2009**, 79, 063203.

(85) Melko, J. J.; Clayborne, P. A.; Jones, C. E.; Reveles, J. U.; Gupta, U.; Khanna, S. N.; Castleman, A. W. Combined experimental and theoretical study of Al_nX (n = 1～6.; X = As, Sb) clusters: evidence of aromaticity and the jellium model. *J. Phys. Chem. A* **2010**, 114, 2045–2052.

(86) Reber, A. C.; Khanna, S. N. Superatoms: electronic and geometric effects on reactivity. *Acc. Chem. Res.* **2017**, 50, 255–263.

(87) Kuo, K. H. Mackay, anti-mackay, double-mackay, pseudo-mackay, and related icosahedral shell clusters. *Struct. Chem.* **2002**, 13, 221–222.

(88) Leuchtner, R. E.; Harms, A. C.; Castleman, A. W. Thermal metal cluster anion reactions - behavior of aluminum clusters with oxygen. *J. Chem. Phys.* **1989**, 91, 2753–2754.

(89) Luo, Z.; Grover, C. J.; Reber, A. C.; Khanna, S. N.; Castleman, A. W. Jr. Probing the magic numbers of aluminum-magnesium cluster anions and their reactivity toward oxygen. *J. Am. Chem. Soc.* **2013**, 135, 4307–4313.

(90) Li, X. L.; Kuznetsov, A. E.; Zhang, H. F.; Boldyrev, A. I.; Wang, L. S. Observation of all-metal aromatic molecules. *Science* **2001**, 291, 859–861.

(91) Luo, Z.; Gamboa, G. U.; Smith, J. C.; Reber, A. C.; Reveles, J. U.; Khanna, S. N.; Castleman, A. W. Jr. Spin accommodation and reactivity of silver clusters with oxygen: the enhanced stability of ag_{13}^-. *J. Am. Chem. Soc.* **2012**, 134, 18973–18978.

(92) Li, J.; Li, X.; Zhai, H. J.; Wang, L. S. Au_{20}: a tetrahedral cluster. *Science* **2003**, 299, 864–864.

(93) Reber, A. C.; Khanna, S. N.; Roach, P. J.; Woodward, W. H.; Castleman, A. W. Jr. Reactivity of aluminum cluster anions with water: origins of reactivity and mechanisms for H–2 release. *J. Phys. Chem. A* **2010**, 114, 6071–6081.

(94) Weichman, M. L.; Debnath, S.; Kelly, J. T.; Gewinner, S.; Schoellkopf, W.; Neumark, D. M.; Asmis, K. R. Dissociative water adsorption on gas-phase titanium dioxide cluster anions probed with infrared photodissociation spectroscopy. *Top. Catal.* **2018**, 61, 92–105.

(95) Pembere, A. M. S.; Liu, X. H.; Ding, W. H.; Luo, Z. X. How partial atomic charges and bonding orbitals affect the reactivity of aluminum clusters with water? *J. Phys. Chem. A* **2018**, 122, 3107–3114.

(96) Zhang, H.; Cui, C.; Luo, Z. The doping effect of 13-atom iron clusters on water adsorption and O-H bond dissociation. *J. Phys. Chem. A* **2019**, 123,

4891–4899.

(97) Chen, J.; Luo, Z. Single-point attack of two H_2O molecules towards a Lewis acid site on the $GaAl_{12}$ clusters for hydrogen evolution. *Chemphyschem* **2019**, 20, 499–505.

(98) Roach, P. J.; Woodward, W. H.; Castleman, A. W. Jr.; Reber, A. C.; Khanna, S. N. Complementary active sites cause size-selective reactivity of aluminum cluster anions with water. *Science* **2009**, 323, 492–495.

(99) Luo, Z.; Smith, J. C.; Woodward, W. H.; Castleman, A. W. Jr. Reactivity of aluminum clusters with water and alcohols: competition and catalysis? *J. Phys. Chem. Lett.* **2012**, 3, 3818–3821.

(100) Luo, Z. X.; Smith, J. C.; Berkdemir, C.; Castleman, A. W. Jr. Gas-phase reactivity of aluminum cluster anions with ethanethiol: carbon-sulfur bond activation. *Chem. Phys. Lett.* **2013**, 590, 63–68.

(101) Luo, Z.; Gamboa, G. U.; Jia, M.; Reber, A. C.; Khanna, S. N.; Castleman, A. W. Jr. Reactivity of silver clusters anions with ethanethiol. *J. Phys. Chem. A* **2014**, 118, 8345–8350.

(102) Luo, Z.; Berkdemir, C.; Smith, J. C.; Castleman, A. W. Jr. Cluster reaction of Ag_8^-/Cu_8^- with chlorine: evidence for the harpoon mechanism? *Chem. Phys. Lett.* **2013**, 582, 24–30.

(103) Reddy, A. S.; Zipse, H.; Sastry, G. N. Cation-pi interactions of bare and coordinatively saturated metal ions: contrasting structural and energetic characteristics. *J. Phys. Chem. B* **2007**, 111, 11546–11553.

(104) Brathwaite, A. D.; Ward, T. B.; Walters, R. S.; Duncan, M. A. Cation-pi and ch-pi interactions in the coordination and solvation of $Au^+(acetylene)_n$ complexes. *J. Phys. Chem. A* **2015**, 119, 5658–5667.

(105) Yang, M.; Wu, H.; Huang, B.; Luo, Z. Cluster-pi interactions cause size-selective reactivity of cationic silver clusters with acetylene: the distinctive Ag_7^+ C_2H_2. *J. Phys. Chem. A* **2019**, 123, 6921–6926.

(106) Han, M.; Wang, Z. Y.; Chen, P. P.; Yu, S. W.; Wang, G. H. Mechanism of neutral cluster beam deposition. *Nucl. Instrum. Methods Phys. Res. Sect. B-Beam Interact. Mater. Atoms* **1998**, 135, 564–569.

(107) Dai, Y.; Gorey, T. J.; Anderson, S. L.; Lee, S.; Lee, S.; Seifert, S.; Winans, R. E. Inherent size effects on xanes of nanometer metal clusters: size-selected platinum clusters on silica. *J. Phy. Chem. C* **2016**, 121, 361–374.

(108) von Weber, A.; Anderson, S. L. Electrocatalysis by mass-selected ptn clusters. *Acc. Chem. Res.* **2016**, 49, 2632–2639.

(109) Timoshenko, J.; Halder, A.; Yang, B.; Seifert, S.; Pellin, M. J.; Vajda, S.; Frenkel, A. I. Subnanometer substructures in nanoassemblies formed from clusters under a reactive atmosphere revealed using machine learning. *J. Phys. Chem. C* **2018**, 122, 21686–21693.

(110) Bentley, C. L.; Kang, M.; Unwin, P. R. Nanoscale surface structure-activity in electrochemistry and electrocatalysis. *J. Am. Chem. Soc.* **2018**, 141, 2179–2193.

(111) Wang, H.; Gu, X. K.; Zheng, X.; Pan, H.; Zhu, J.; Chen, S.; Cao, L.; Li, W. X.; Lu, J. Disentangling the size-dependent geometric and electronic effects of palladium nanocatalysts beyond selectivity. *Sci. Adv.* **2019**, 5, eaat6413.

(112) Zhou, M.; Bao, S.; Bard, A. J. Probing size and substrate effects on the hydrogen evolution reaction by single isolated pt atoms, atomic clusters, and nanoparticles. *J. Am. Chem. Soc.* **2019**, 141, 7327–7332.

(113) Yin, C.; Negreiros, F. R.; Barcaro, G.; Beniya, A.; Sementa, L.; Tyo, E. C.; Bartling, S.; Meiwes-Broer, K. H.; Seifert, S.; Hirata, H.; Isomura, N.; Nigam, S.; Majumder, C.; Watanabe, Y.; Fortunelli, A.; Vajda, S. Alumina-supported sub-nanometer Pt10 clusters: amorphization and role of the support material in a highly active co oxidation catalyst. *J. Mater. Chem. A* **2017**, 5, 4923–4931.

(114) Yang, B.; Liu, C.; Halder, A.; Tyo, E. C.; Martinson, A. B. F.; Seifer, S.; Zapol, P.; Curtiss, L. A.; Vajda, S. Copper cluster size effect in methanol synthesis from CO_2. *J. Phys. Chem. C* **2017**, 121, 10406–10412.

(115) Halder, A.; Liu, C.; Liu, Z.; Emery, J. D.; Pellin, M. J.; Curtiss, L. A.; Zapol, P.; Vajda, S.; Martinson, A. B. F. Water oxidation catalysis via size-selected iridium clusters. *J. Phys. Chem. C* **2018**, 122, 9965–9972.

(116) Halder, A.; Curtiss, L. A.; Fortunelli, A.; Vajda, S. Perspective: size selected clusters for catalysis and electrochemistry. *J. Chem. Phys.* **2018**, 148, 110901.

(117) Laskin, J.; Johnson, G. E.; Warneke, J.; Prabhakaran, V. From isolated ions to multilayer functional materials using ion soft landing. *Angew Chem. Int. Ed. Engl.* **2018**, 57, 16270–16284.

(118) Lei, Y.; Mehmood, F.; Lee, S.; Greeley, J.; Lee, B.; Seifert, S.; Winans, R. E.; Elam, J. W.; Meyer, R. J.; Redfern, P. C.; Teschner, D.; Schlogl, R.; Pellin, M. J.; Curtiss, L. A.; Vajda, S. Increased silver activity for direct propylene epoxidation via subnanometer size effects. *Science* **2010**, 328, 224–228.

(119) Cui, C.; Luo, Z.; Yao, J. Enhanced catalysis of pt3 clusters supported on graphene for N–H bond dissociation. *CCS Chemistry* **2019**, 1, 215–225.

(120) Zhang, H.; Cui, C.; Luo, Z. MoS_2-supported Fe_2 clusters catalyzing nitrogen reduction reaction to produce ammonia. *J. Phy. Chem. C* **2020**, 124, 6260–6266.

(121) Qin, Y.; Han, J.; Guo, G.; Du, Y.; Li, Z.; Song, Y.; Pi, L.; Wang, X.; Wan, X.; Han, M.; Song, F. Enhanced quantum coherence in graphene caused by Pd cluster deposition. *Appl. Phys. Lett.* **2015**, 106, 023108.

(122) Kwon, G.; Ferguson, G. A.; Heard, C. J.; Tyo, E. C.; Yin, C.; DeBartolo, J.; Seifert, S.; Winans, R. E.; Kropf, A. J.; Greeley, J.; Johnston, R. L.; Curtiss, L. A.; Pellin, M. J.; Vajda, S. Size-dependent subnanometer pd cluster (Pd–4, Pd–6, and Pd–17) water oxidation electrocatalysis. *Acs Nano* **2013**, 7, 5808–5817.

(123) Miller, S. A.; Luo, H.; Pachuta, S. J.; Cooks, R. G. Soft-landing of polyatomic ions at fluorinated self-assembled monolayer surfaces. *Science* **1997**, 275, 1447–1450.

(124) Mitsui, M.; Nagaoka, S.; Matsumoto, T.; Nakajima, A. Soft-landing isolation of vanadium-benzene sandwich clusters on a room-temperature substrate using n-alkanethiolate self-assembled monolayer matrixes. *J. Phys. Chem. B* **2006**, 110, 2968–2971.

(125) Nesselberger, M.; Roefzaad, M.; Hamou, R. F.; Biedermann, P. U.; Schweinberger, F. F.; Kunz, S.; Schloegl, K.; Wiberg, G. K.; Ashton, S.; Heiz, U.; Mayrhofer, K. J.; Arenz, M. The effect of particle proximity on the oxygen reduction rate of size-selected platinum clusters. *Nat. Mater.* **2013**, 12, 919–924.

(126) Wettergren, K.; Schweinberger, F. F.; Deiana, D.; Ridge, C. J.; Crampton, A. S.; Rotzer, M. D.; Hansen, T. W.; Zhdanov, V. P.; Heiz, U.; Langhammer, C. High sintering resistance of size-selected platinum cluster catalysts by suppressed ostwald ripening. *Nano Lett.* **2014**, 14, 5803–5809.

(127) Rondelli, M.; Zwaschka, G.; Krause, M.; Rötzer, M. D.; Hedhili, M. N.; Högerl, M. P.; D'Elia, V.; Schweinberger, F. F.; Basset, J. M.; Heiz, U. Exploring the potential of different-sized supported subnanometer pt clusters as catalysts for wet chemical applications. *ACS Catal.* **2017**, 7, 4152–4162.